Accepted Manuscript

Heat pipe-based radiator for low grade geothermal energy conversion in domestic space heating

K. Kerrigan, H. Jouhara, G.E. O'Donnell, A.J. Robinson

PII: S1569-190X(10)00121-8
DOI: 10.1016/j.simpat.2010.05.020
Reference: SIMPAT 957

To appear in: *Simulation Modeling Practices and Theory*

Received Date: 16 October 2009
Revised Date: 21 May 2010
Accepted Date: 31 May 2010

Please cite this article as: K. Kerrigan, H. Jouhara, G.E. O'Donnell, A.J. Robinson, Heat pipe-based radiator for low grade geothermal energy conversion in domestic space heating, *Simulation Modeling Practices and Theory* (2010), doi: 10.1016/j.simpat.2010.05.020

HEAT PIPE-BASED RADIATOR FOR LOW GRADE GEOTHERMAL ENERGY CONVERSION IN DOMESTIC SPACE HEATING

K. Kerrigan[1], H. Jouhara[2], G.E. O'Donnell[1], A. J. Robinson[1*]

[1]Department of Mechanical & Manufacturing Engineering, Parsons Building, Trinity College Dublin 2, Ireland; email: arobins@tcd.ie

[2]School of Engineering and Design, Brunel University, Uxbridge, Middlesex, UB8 3PH, UK, Tel: +44 1895 267656, Fax: +44 1895 256392, Email: hussam.jouhara@brunel.ac.uk

ABSTRACT

A severe technical drawback of geothermal heat pumps (GHPs) is the fact that the nominal operating temperature available for domestic space heating is typically in the region of 50°C. This is 25°C to 40°C less than conventional boiler settings used in hydronic central heating applications. As a result, GHPs are not generally ideal for direct replacement of conventional hydronic central heating systems because of the low relative distribution temperatures unless extreme measures are taken to improve the thermal insulation of the buildings. A preferable option for GHPs is underfloor heating. In terms of retrofitting existing buildings neither the re-insulating nor the underfloor heating options are attractive due to the large added cost and disruptive nature of the installation. As such, very high performance low temperature radiators that are pluggable into existing hydronic central heating systems are a major enabling technology for this sustainable energy source. In this investigation a Simulation Driven Design technique was utilized to develop a novel low water content and high thermal throughput heat pipe-based radiator. The radiator was subsequently fabricated and tested and showed an exceptionally high power density and very fast response time compared with conventional wet radiators.

Keywords: Heat Pipe, Heat Exchanger, Design

1 INTRODUCTION

Conventional heat exchangers (HEXs) for hydronic central heating applications have changed very little over the past one hundred years or more. In these types of units, the hot source water flow is channelled within the HEX. In this way, hot fluid comes into contact with a large enough internal surface area within the device to allow the required amount of heat to be dissipated passively into the room by buoyant natural convection and radiation. Newer devices operate on the same principle though may include external fins to decrease the overall size and weight of the units. The main drawbacks of having the hot water flowing within a large internal volume are: that the devices are unnecessarily large and/or must operate with high source water temperatures, typically above 70ºC [1]; the water cools as it crosses the HEX causing large temperature variations across it (the cooler regions dissipate less heat requiring the HEX to be longer to achieve rated power); due to the very slow moving water within the HEX, the air which is dissolved within the water collects within the device forming air pockets. These air pockets have the effect of making the effective heat dissipating area smaller i.e. operating below design specification, requiring frequent bleeding to dispel the air. Finally, the combination of the fact

* Corresponding author. Phone: +353 1 856 3919, e-mail: arobins@tcd.ie (Anthony Robinson)

that the surface area must be large enough to reach a given power dissipation and that the entire unit must have a built strength to withstand over 8 bar operating pressure results in very heavy HEXs that has the negative influence of taking a substantial time to heat to operating temperature/power level. The large mass of material combined with the large volume of water has a major adverse impact on start-up as well as the thermostatic control capability and room comfort.

Conventional radiators are not ideal for use in geothermal heat pump (GHP) domestic heating applications because of the low source water temperatures generated. The power densities are typically so low that massively oversized radiators would be required. A preferable option for GHPs is enhanced building insulation or under floor heating systems. In terms of retrofitting existing buildings neither the re-insulating nor the under floor heating options are attractive due to the large added cost and disruptive nature of the installation [1].

Building legislation and environmental concerns [2-4] are driving designers of building services and air conditioning systems towards more energy efficient solutions such as heat pipes. Heat pipe technology has proven track records in space technology [5, 6], thermal storage [7, 8], harnessing of renewable energy [9-10] and in waste heat recovery of various processes [11, 12]. In domestic air conditioning systems, its advantages and economics are proven [13] with an expanding number of applications, which utilise such technology to ensure that energy is transferred in an efficient way [13-15].

In the current investigation a novel high power density radiator for hydronic central heating applications has been developed that utilizes heat pipes. A heat pipe is a hermetically sealed tube that contains a small amount of fluid, which exists inside the heat pipe shell as vapour and liquid at equilibrium [16]. When heat is applied at one end of a heat pipe the liquid within it evaporates. The heat transfer rate within the wick structure is extremely high as it is a combination of conduction across a very thin saturated metallic wick and or nucleate boiling [17]. The vapour which is generated at the heated end spreads to the cooled end of the heat pipe. Here the extraction of energy causes the vapour within the heat pipe to condense back to a liquid phase thus releasing the heat that was absorbed at the heated region albeit at a different location, i.e. at some location remote from the heated end. A porous wick structure wrapped around the inner wall of the heat pipe draws the liquid condensate back to the heated section where it is once again vaporized. In the current investigation, water was chosen as the working fluid and copper as the shell material. As water and copper are chemically compatible, no generation of non condensable gasses (NCGs) will be taking place within the heat pipe [18, 19]. The generation of NCGs typically has an adverse affect on the performance of a heat pipe as the NCGs accumulate in the condenser section of the heat pipe subsequently reducing the length of heat pipe capable of releasing the latent heat of vaporisation.

To achieve the power density required for effective heat dissipation from low grade geothermal heat sources a Simulation Driven Design technique was implemented which utilized commercial computational fluid dynamics (CFD) software to model the convective and radiative heat transport of a single channel of the finned heat pipe tube bundle immersed in otherwise quiescent room temperature air. The purpose of the CFD simulations in this work was therefore to accelerate the design process by allowing multiple geometric configurations to be considered in terms of single phase air side heat transfer capabilities. This meant that while experimental works were later carried out to ensure the validity of the final design, the effectiveness of that final design relative to other pipe configurations and fin spacings could be considered prior to the prototyping/experimental phase of the works.The radiator as well as a test facility was subsequently fabricated and the results compared favourably with simulations. Further, the steady and transient responses were tested against a standard commercially available radiator to illustrate the improved thermal performance.

2 DESIGN CONCEPT

The design concept of the heat pipe-based radiator is given in Fig. 1. As illustrated in the figure, one end of the heat pipes is immersed in the flow of hot source water at the collector end of the HEX called the hot water manifold. Here the heat energy of the hot source water flow is absorbed into the six heat pipes by vaporising the water inside them. Since they are under a partial vacuum the water within them boils at a temperature that is lower than the source hot water temperature.

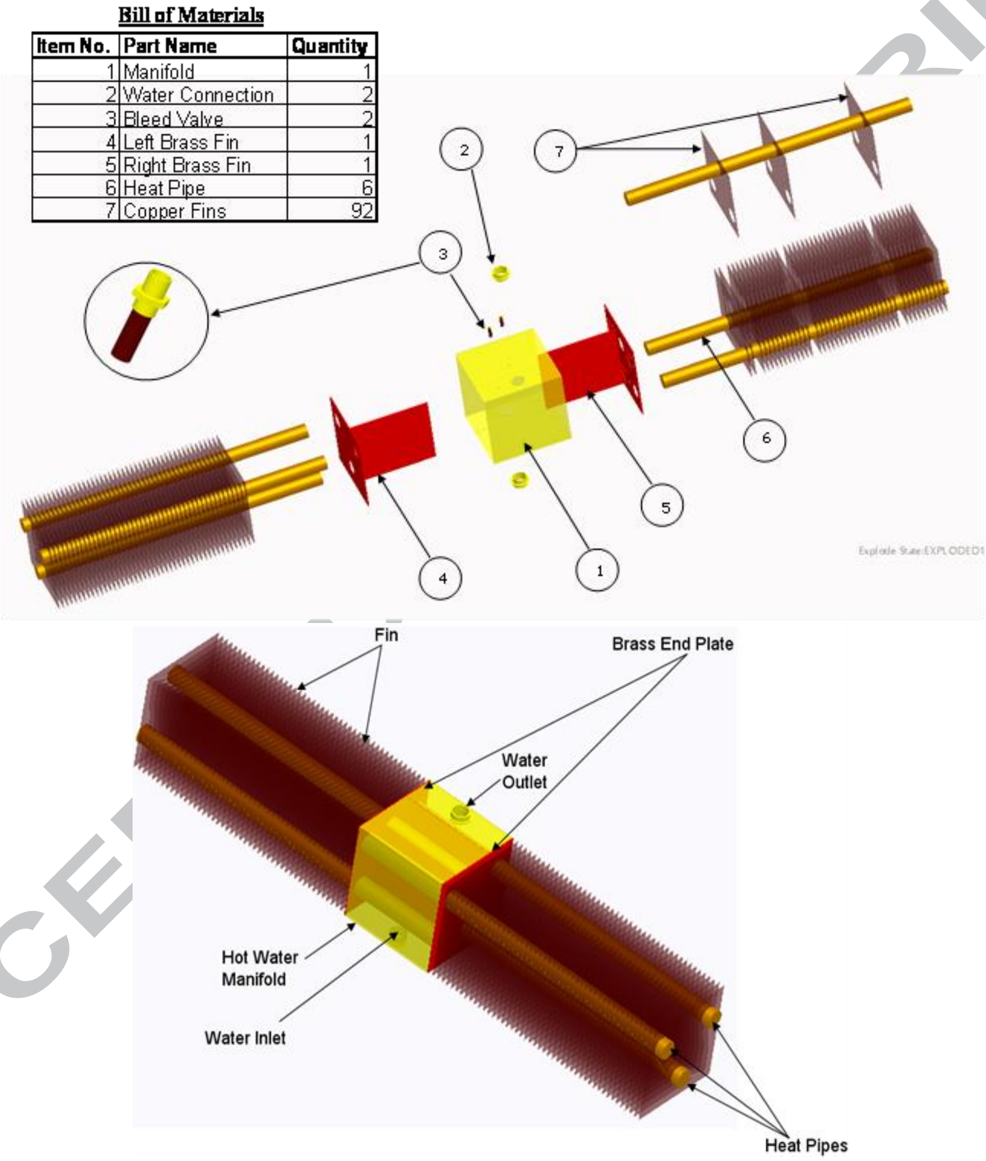

Figure 1: Schematic of double convector heat pipe-based heat exchanger (top) assembly drawing (bottom) assembled unit.

As depicted in Fig. 1 there are dividing plates within the manifold which force the water over the collector ends of the heat pipes within a serpentine channel for improved thermal energy transfer. The steam generated inside the heat pipes at the collector end flows away from the collector region of the heat pipes to the heat ejector end. Here it condenses on the inner wall of the heat pipes releasing the heat at a location which is remote from where it was absorbed. In the heat ejector region the outer surface of the heat pipes are fitted with simple metallic fins (i.e. surface extensions) to achieve the necessary power dissipation for the given operating temperature. In the heat ejector region, referred to as a finned tube bundle, the location of the heat pipes and the spacing between the fins has been designed for optimal heat transfer by buoyant natural convection and thermal radiation.

3 SIMULATION DRIVEN DESIGN

Due to the complex nature of the flow and heat transfer within the finned tube bundle, conventional correlations for natural convection are not sufficiently accurate for design purposes. This being the case, a Simulation Driven Design (SDD) technique was implemented whereby the commercial CFD package ANSYS CFX was utilised to simulate the coupled flow and heat transfer within a single channel of the fin bank. The physical domain in this analysis incorporates the assumed isothermal condenser section of the heat pipe(s), the metallic fin attached to the heat pipe and the section of air between the fins and surrounding the heat pipe(s). The isothermal nature of the heat pipes, the repetitive nature of the fin spacing, in combination with the geometric symmetry inherent in the circular tube structures allowed for the use of only one quarter of the overall physical model during analysis (half in the vertical direction and half in the thickness). Such simplifications of the physical model lead to large reductions in computation time. Due to the isothermal nature of heat pipes, the current analysis results were therefore used to determine the power throughput of all channels in the heat dissipating (condenser) region of the HEX. From such results, design aspects such as size and spacing of the fins and tubes were then varied to achieve the desired thermal performance. The CFD code solved the three dimensional equations for continuity, momentum and energy to simulate the thermal and flow fields for the incompressible, steady state *'natural convection in air'* model as follows:

$$\frac{\partial u}{\partial x}+\frac{\partial v}{\partial y}+\frac{\partial w}{\partial z}=0 \tag{1}$$

$$\rho\left(u\frac{\partial u}{\partial x}+v\frac{\partial u}{\partial y}+w\frac{\partial u}{\partial z}\right)=-\frac{\partial p}{\partial x}+\mu\nabla^2 u \tag{2}$$

$$\rho\left(u\frac{\partial v}{\partial x}+v\frac{\partial v}{\partial y}+w\frac{\partial v}{\partial z}\right)=-\frac{\partial p}{\partial y}+\mu\nabla^2 v-\rho g \tag{3}$$

$$\rho\left(u\frac{\partial w}{\partial x}+v\frac{\partial w}{\partial y}+w\frac{\partial w}{\partial z}\right)=-\frac{\partial p}{\partial z}+\mu\nabla^2 w \tag{4}$$

$$u\frac{\partial T}{\partial x}+v\frac{\partial T}{\partial y}+w\frac{\partial T}{\partial z}=\alpha\nabla^2 T \tag{5}$$

In the above set of Navier-Stokes equations, u, v and w represent the x, y and z directional components of air velocity, ρ represents the air density, p is the air pressure, μ is the dynamic viscosity of the air and g is the gravitational constant.

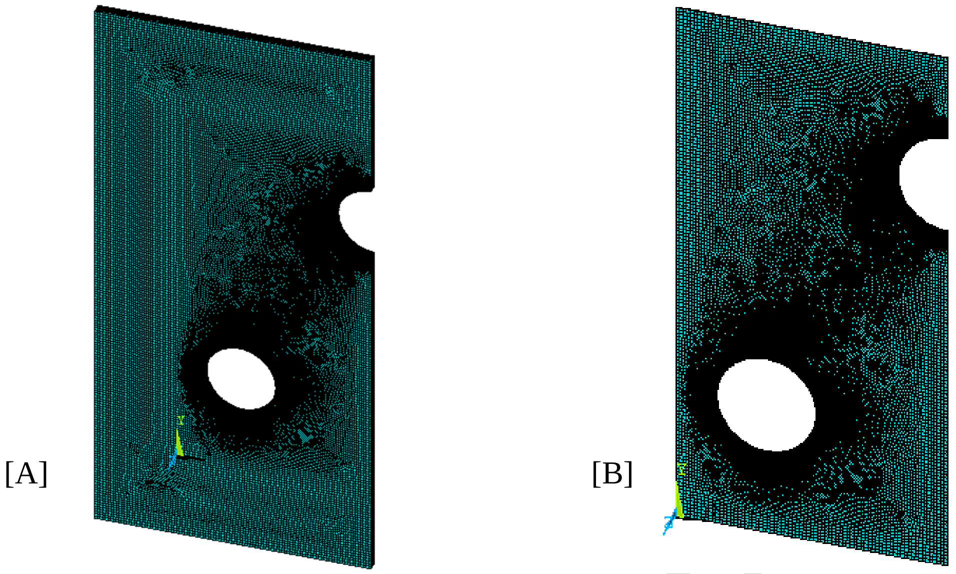

Figure 2: Example of the meshed elemental structure for both the [A] air and [B] fin models.

The mesh used to generate the domains for the fin and air channel are shown in fig. 2. Two separate models were meshed using the ANSYS 11.0 meshing facility and imported into ANSYS CFX as .cdb files.

Holes of radius, R_p, 13.7mm (representative of where the ¾ inch copper heat pipes would be placed) were positioned at coordinates (L_f/6,H_f/4) and (L_f/2,3H_f/4) in each model. For the air channel model, both the length, L_f, and height, H_f, of the fin model were increased by 20 percent. This was done to ensure that the analysis included heat transfer effects within the air channel which exceeded the geometry of the fin.

Due to large temperature gradients in the region of the heat pipe representative section of the models, grid clustering was implemented in these regions as seen by the dense mesh surrounding the holes of each model in fig. 2. A separate, diametric mesh boundary region, 20 percent larger than the heat pipe hole diameter, was generated to encompass the area perpendicular to the axis of the heat pipe. The 20 percent larger circumferential lines were divided into 150 segments to facilitate a fine tetrahedral mesh, generating 8,050 quadrilateral elements in each model. The external edge length for the fin and air were then set to 1mm and 3mm respectively and a free quadrilateral mesh resulted in 53,894 & 311,715 quadrilaterals for the respective models.

Two domains were created for this analysis, a fluid (for the air channel) and a solid (for the fin) model. The fluid model incorporated default CFX properties for air at room temperature with the exception of density. The equation for dry air density was used to generate air density as a function of temperature:

$$\rho = \frac{p_{prescribed}}{R \cdot T} \qquad (6)$$

Where ρ is the air density

p is atmospheric pressure (1.013 x 10^5 Pa)

R is the gas constant for air (287.058 J/kgK)

T is the temperature (K)

The utilization of a temperature dependent density allowed for the full buoyancy model to be incorporated into the analysis, whereby $\rho - \rho_{ref}$ was evaluated directly for each analysis node. The reference density, ρ_{ref}, was set at 1.20403 kg/m^3 for the air domain.

For heat transfer within the fluid domain, the built-in thermal energy model of CFX was used, as described in eq. (3). The initial conditions for this domain were:

$$U = 0\ \frac{m}{s} \qquad V = 0\ \frac{m}{s} \qquad W = 0\ \frac{m}{s} \qquad P_{rel} = 0\ \text{Pa} \qquad T = 20°\text{C}$$

For the solid domain, the default values in CFX for copper were used. The heat transfer mechanism was also set to thermal for this domain. The initial conditions for the copper fin were:

$$T = 20°\text{C}$$

The monte carlo radiation model was used for this analysis. Emissivity values of 0.77 and 1 were used for the fin (solid domain) and air channel (fluid domain) respectively, while the diffuse fraction value was left as 1 for both domains.

Fig. 3 indicates several boundary conditions which were applied. It indicates four axes of symmetry (two in each model view – one in the central vertical plane of the side view and one in the central vertical plane of the elevation view). These are denoted by green dashed vertical lines and '*sym*'. The air not overlapping or interfacing with the solid domain, i.e. exterior to the fin channel, was also given a symmetry boundary condition, denoted by brown dotted vertical lines and '*Air Sym*'.

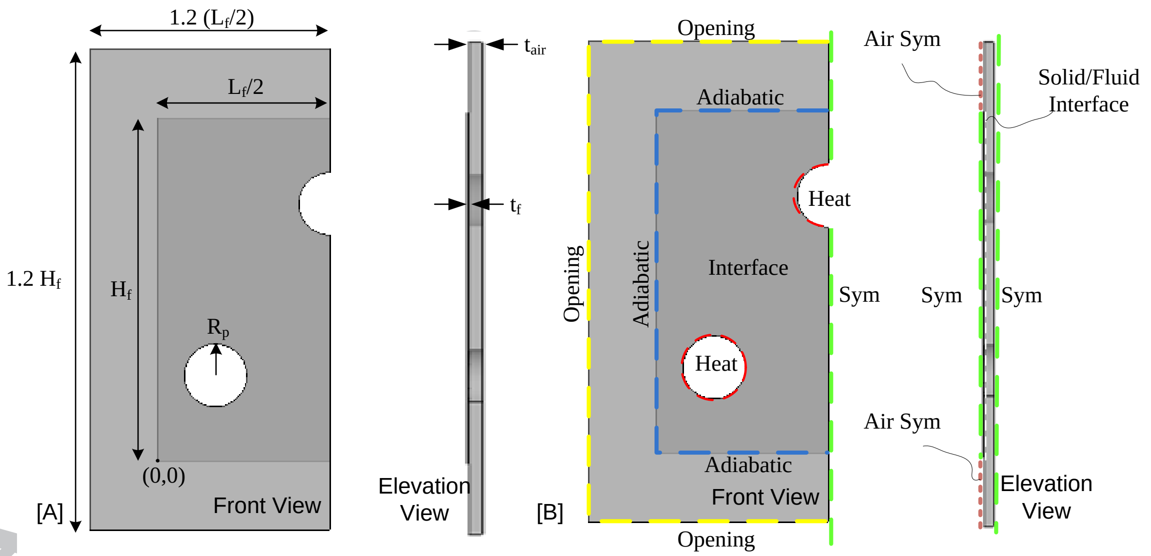

Figure 3: [A] Side view (left) and elevation (right) of the domains in ANSYS CFX indicating the geometric values used, and [B] Side view (left) and elevation (right) of the domains indicating the various boundary conditions placed on the models prior to running the solver.

The outer walls of the Air, denoted by yellow lines were given an opening boundary condition allowing fluid to cross the boundary surface in either direction. A subsonic flow regime was utilised, whereby an assumption was made that air, under natural convection, is incompressible and low-speed. The direction for flow was set normal to the boundary and a relative opening pressure of 0 Pa was used. This value was interpreted as the relative total pressure for the inflow and relative static pressure for outflow at this boundary. The static boundary temperature was set at a standard room temperature of 20°C.

The outer walls of the fin were given an adiabatic boundary along the thickness of the wall. In this case the heat flux across the wall boundary is zero, i.e insulated. This assumption was based on the fact that the wall thickness was significantly smaller than the other geometric values.

A fixed temperature, i.e. a '*Heat'* wall boundary condition, was specified for the surface inside the thickness of both holes in the fin and air models. This was done in order to simulate the relatively isothermal nature of the heat pipes.

A domain interface was required for this analysis due to the use of multiple domains (air channel and fin). In this case there was a fluid-solid interface set up. A general connection was used to connect the regions due to the non-matching grids of the two regions. A general grid interface (GGI) tool within CFX was utilised due to potentially non-matching node locations, element types and flow physics across the connection between air and fin. This connection method was selected over direct (one-to-one) connections since in fluid-solid interfaces within ANSYS CFX, the direct connection uses a non-symmetric discretisation of heat flow through the assembly of models, i.e. direct connections use more information from the more conductive side of the interface, while GGI connections sample both regions equally.

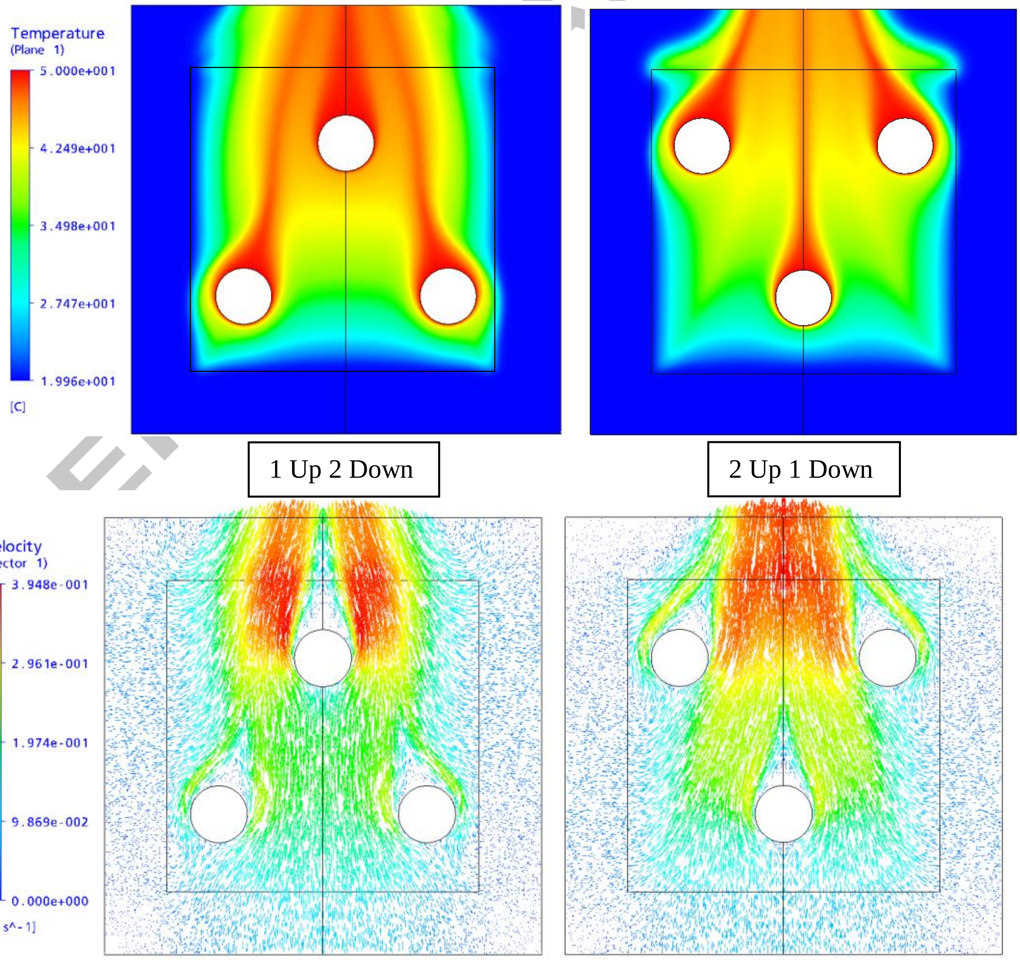

Figure 4: Simulations for 50°C heat pipe wall temperature. *Top*: the temperature profile through the centre of the air channel of both 1 up 2 down and 2 up 1 down tube configurations. *Bottom*: Vector plot of the velocity of the air in the centre of the channel.

The product of the averaged heat flux values and the surface area of the solid-fluid interface allowed for the heat power throughput to be determined for the finned-tube channel. Multiplying this heat power by a number suitable for the number of symmetries associated with the model (i.e. if 2 planes of symmetry were employed then the multiplier is 2) yields the total heat power (W) of a single channel of the HEX. Since the condenser section of the heat pipe is assumed isothermal, this was used to determine the overall performance (in terms of heat power output) of the HEX design.

The Simulation Driven Design (SDD) methodology was implemented to determine the ideal channel width and location of the heat pipes for a constrained fin dimension of 15 cm x 15 cm. The fin thickness was confined to 0.5mm thick copper sheet in order to ensure both a robust design and to minimise the heat released from the thickness of the fin, thus allowing the adiabatic assumption/boundary condition to be applied.

Fig. 4 illustrates an example of the simulated flow and thermal fields along the centreline of the final channel arrangement for the case of a 50°C heat pipe wall temperature for both the 1 up 2 down and 2 up 1 down heat pipe configurations.

The SDD process indicated that the staggered arrangement improved the net power output of the channel compared with in-line configurations due to flow blockage by the downstream tubes. Increasing the centre-to-centre distance (pitch) of the tubes tended to improve the heat transfer to a point at which the heat transfer was maximised, since as the tubes approached the outer edge of the fins, the heat spreading within the fins began to deteriorate.

The simulated power throughput per channel is given in Fig. 5 for increasing heat pipe wall temperature. It is evident that there is a near linear dependence of the heat transfer rate with wall temperature for the range of temperatures investigated. For a wall temperature of 50°C, roughly that of the source water of a GHP, the channel is predicted to dissipate about 4.7W. Generally, 10% of the total heat transfer was predicted to be due to radiation with the remaining by buoyant natural convection. It is also evident that the 1 up 2 down arrangement tends to outperform the 2 up 1 down arrangement, albeit marginally.

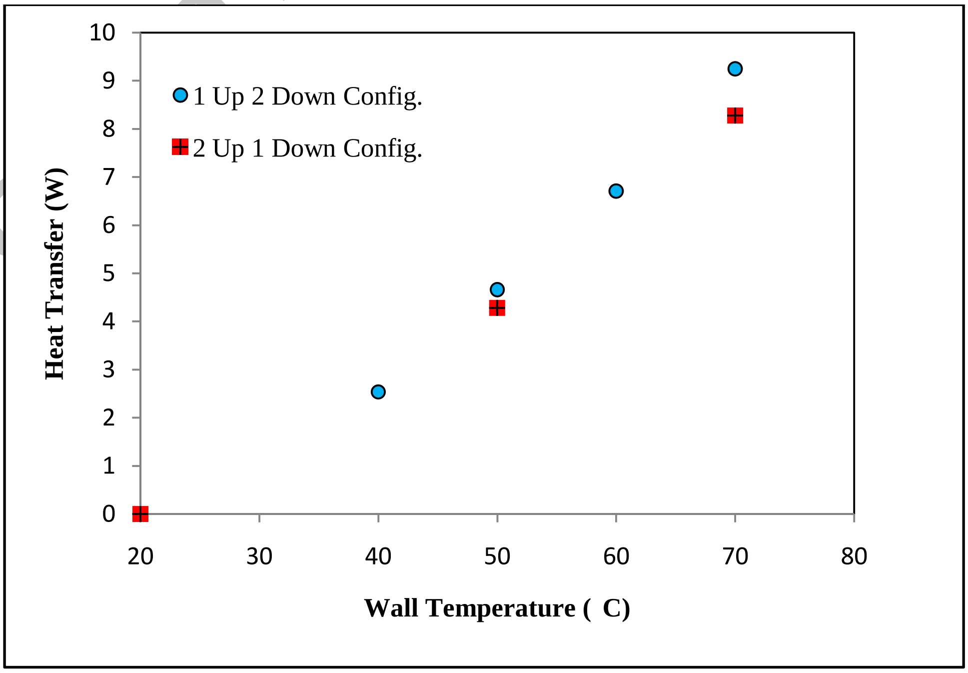

Figure 5: Heat transfer rate versus heat pipe wall temperature for a single channel for ambient temperature of 20°C.

4 HEX FABRICATION AND TEST FACILITY

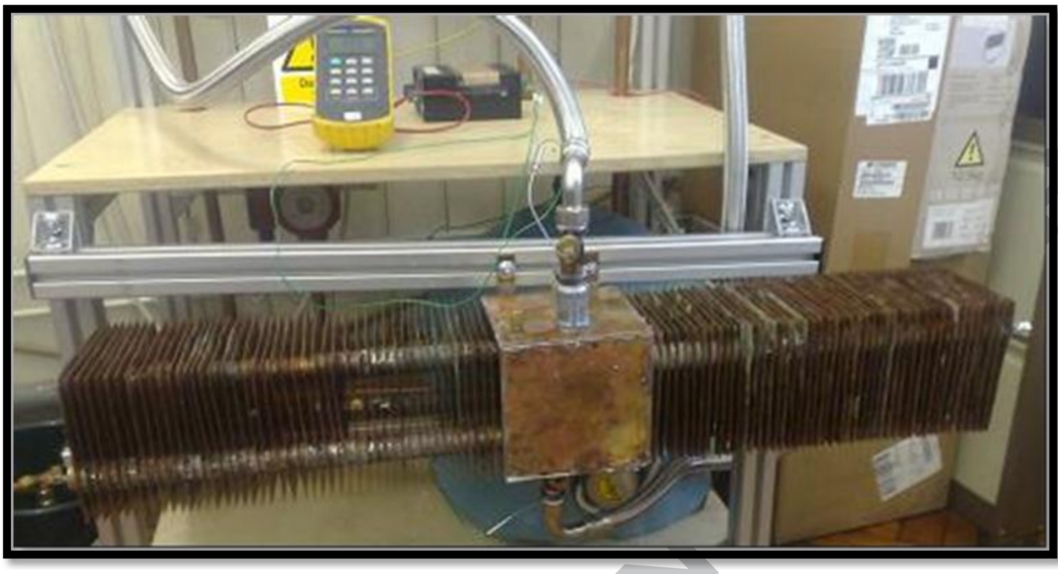

Figure 6: Heat pipe radiator prototype

A prototype heat pipe radiator was fabricated in-house and is shown in Fig. 6. It is the physical embodiment of what is depicted in Fig. 1. The convector consists of 6 water charged heat pipes of 55.6 cm length and 27.4 cm diameter. The interior of the heat pipes are lined with 3 wraps of MESH145 copper screen mesh. The heat collector end is 15 cm long and the heat ejector ends are 40 cm long and each fitted with 46 15 cm x 15 cm copper fins of 0.5 mm thickness. The inner part of the pipe consisted of 12ml of water surrounded completely by a vacuum, with three diametric wraps of MESH145 copper wick structure gripping the internal surface of the hermetically sealed copper pipe. The overall volume of the HEX is 1.603 x 10^{-3} m^3.

A thermal performance test facility was constructed to evaluate the overall performance of the radiator. The main features of the test rig are illustrated in Fig. 7. A circulation pump draws hot water from a storage tank fitted with electrical immersion heaters. The heaters are wired to a control box that regulates the water temperature to a preset value.

The volume of flow is controlled by a simple bypass valve and is measured with an in-line flow meter. Flexible hoses are then fixed to the inlet and outlet fitting of the radiator being tested. Thermocouples are placed in the hot water flow at the inlet and outlet of the radiator.

The power, P, dissipated by the radiator is related to the volumetric flow rate of the water and the net temperature drop across the radiator unit through the equation:

$$P = \rho \dot{V} (T_{w,In} - T_{w,Out}) \quad (7)$$

where ρ is the water density and $\dot{V}$ is the water volumetric flow rate. The figure of merit for comparing different radiators of different overall volume, *V*, is related to the measured power density, given by:

$$PD = {}^{P}\!/_{V} \quad (8)$$

for a given water-to-room temperature differential:

$$\Delta T = T_{w,In} - T_{Room} \quad (9)$$

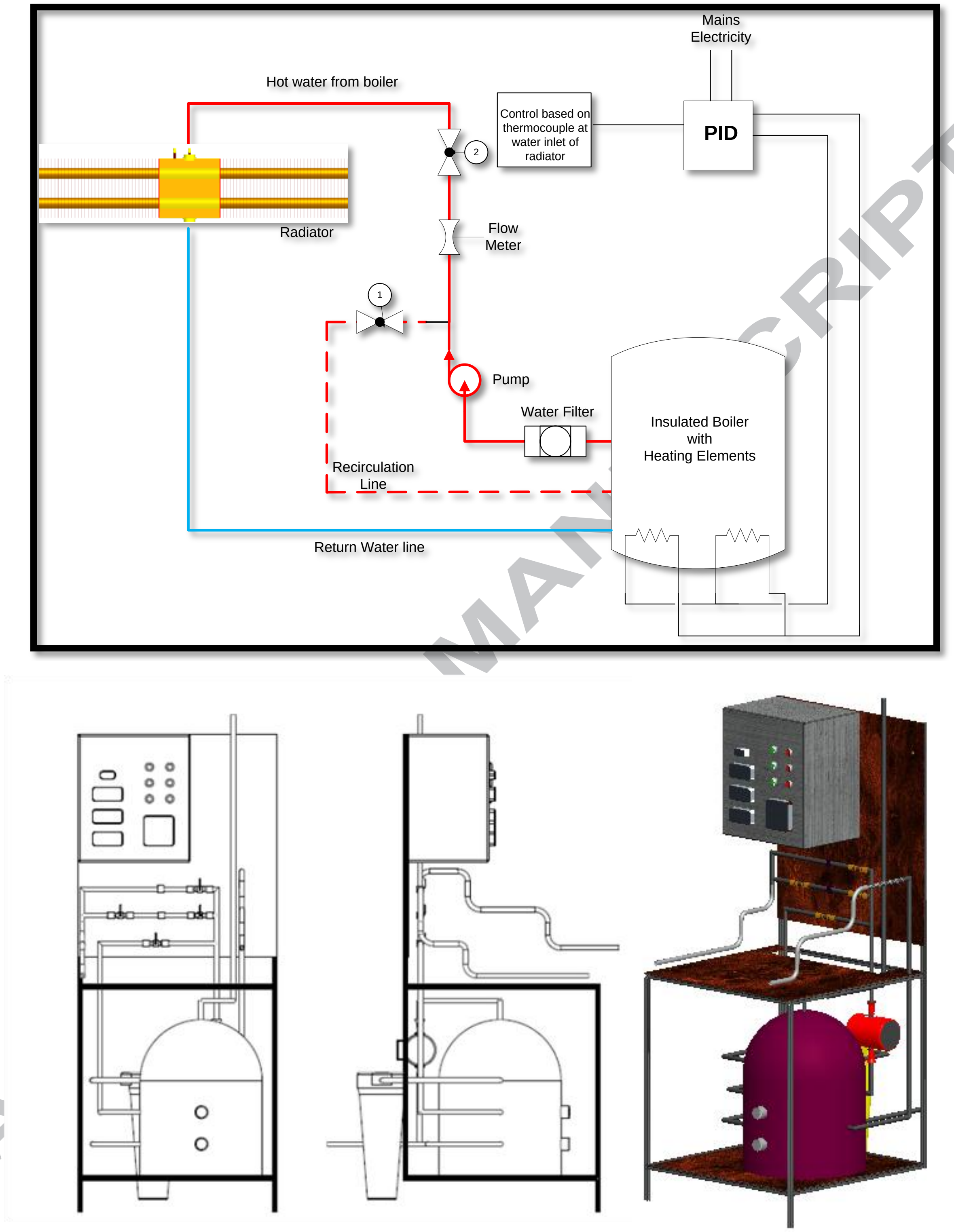

Figure 7: *(Top)* Schematic of thermal performance characterization test facility. *(Bottom)* CAD renders of the test facility.

Fig. 8 shows a thermal image of the heat pipe prototype for a water inlet temperature of 70°C. It is evident that the heat pipes distribute the heat relatively evenly along the finned tube bank which is ideal. It should be noted that the surface emissivity is non-uniform due to the manufacturing procedure and it was not feasible to paint the entire HEX.

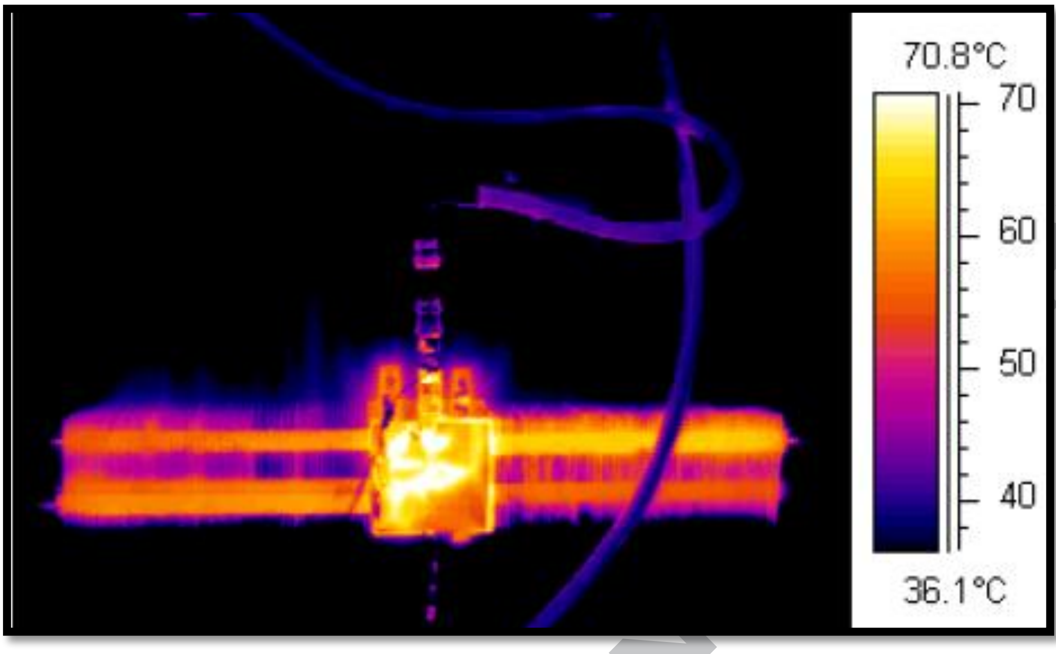

Figure 8: Thermal image of heat pipe prototype radiator.

The net heat transfer rate for increasing inlet water temperature for the prototype heat pipe-based domestic radiator is depicted in Fig. 9 along with the simulation predictions for increasing heat pipe wall temperature. The experimental results include the heat transfer from the collector manifold located at the centre of the unit, which is in the region of 50 W. Taking this into account it is apparent that there is adequate agreement between the experimental results and the CFD simulations. The CFD simulations consistently under predict the heat transfer rate by about 5% to 10%, which is within the experimental uncertainty of the measured results.

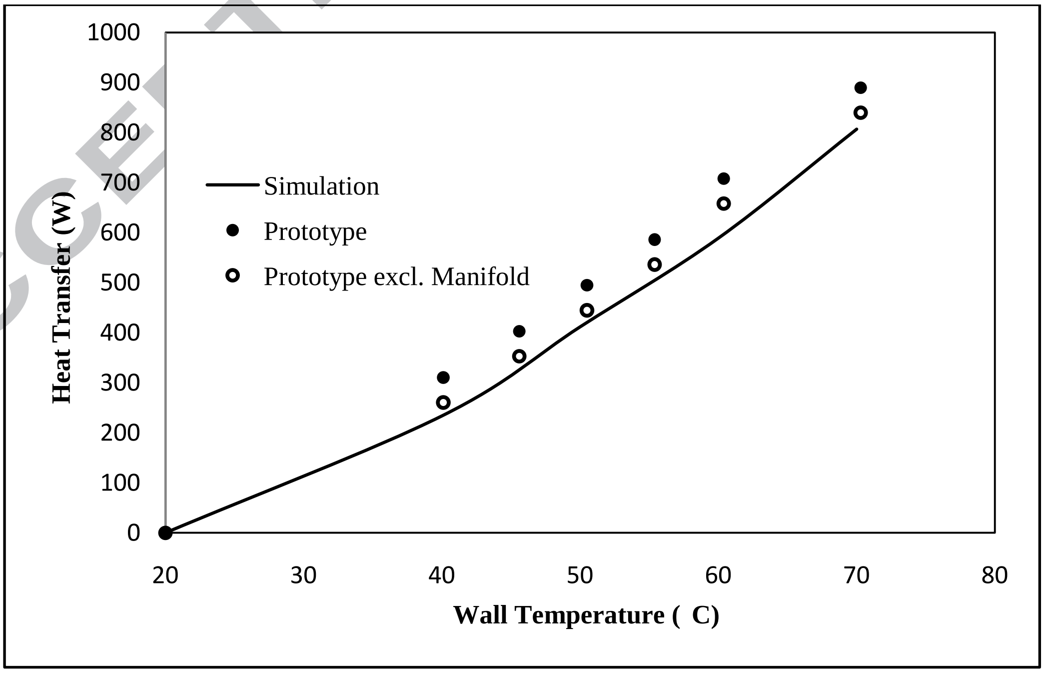

Figure 9: Power output versus water inlet temperature / wall temperature comparing experimental prototype with simulations for ambient temperature of 20°C.

With regard to overall output the prototype can transfer approximately 500W at a water source temperature of 50°C increasing to 900 W for a water source temperature of 70°C.

Perhaps a better measure of the performance of the prototype is to compare its power density characteristics versus a popular conventional domestic radiator. This is depicted in Fig. 10 where it is clear that with regard to power output per unit volume, the heat pipe prototype outperforms a conventional radiator by a factor of about two, which is substantial.

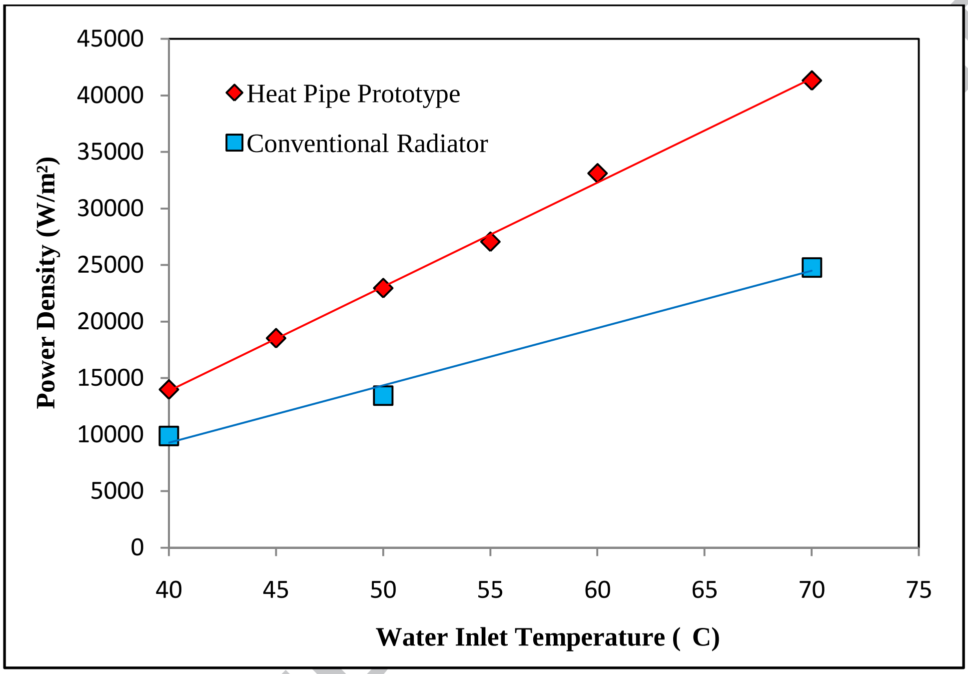

Figure 10 Experimental results: Power density versus temperature for the heat pipe prototype and a popular off the shelf domestic radiator.

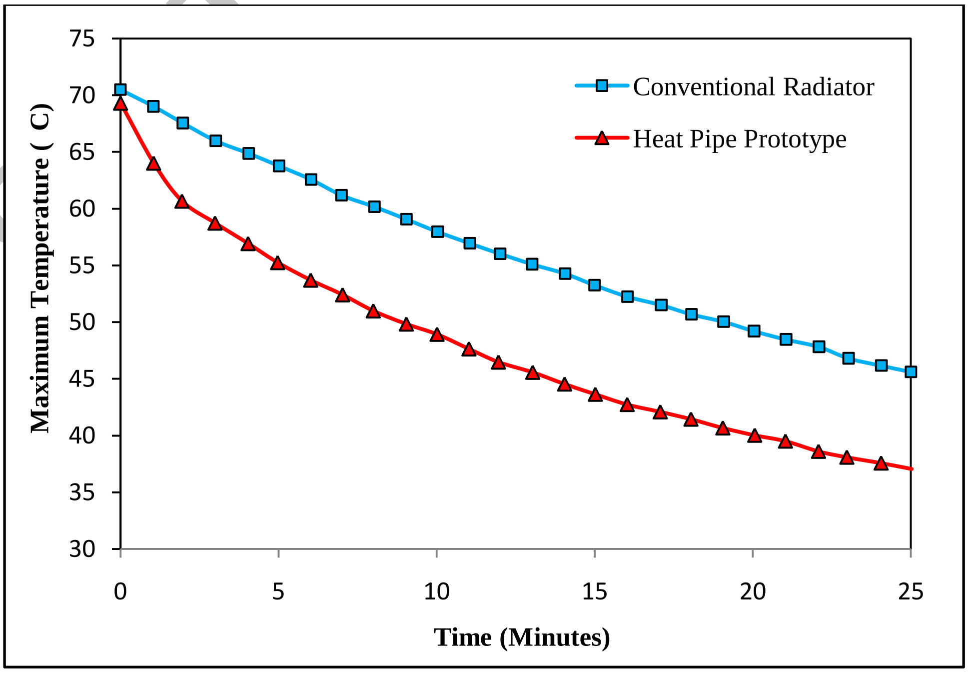

Figure 11 Maximum temperature versus time subsequent to an abrupt stoppage in water flow during experimentation.

Another novel aspect of the heat pipe design concept is that there is virtually no water within the heat dissipating region i.e. within the condenser end of the heat pipe. As a result, when the water flow is ceased and the water side thermal resistance becomes so large as to severely reduce the heat transfer capability of the HEX, the heat dissipating end cools very quickly due to the low water content of this region. This is illustrated in Fig. 11. Here a simple test was performed whereby the inlet valve was closed and the maximum temperature history was recorded with the thermal imaging camera. It is clear from the figure that the heat pipe prototype cools considerably faster than the popular off the shelf unit as the later includes the thermal mass of the water trapped within it which is considerable. To gauge the difference the initial 10^{o}C drop in temperature takes 8 minutes in the conventional unit and only 2 minutes with the heat pipe radiator which is a notable improvement.

5 CONCLUSIONS AND OUTLOOK

The prototype heat pipe based double convector radiator has proven the concept that using heat pipes as heat spreaders for effective heat dissipation in domestic applications has many advantage over conventional wet panel radiators, including a doubling of the power density and significantly reduced thermal mass for improved controllability. The novelty of the overall design is mainly seen in single phase extended surface designs associated with this device and the ability of the heat pipe to efficiently transport heat from the source water to the ambient environment. In the liquid (water) phase, the use of serpentine channels in order to allow a more controlled flow over the heat pipes has not been done in radiator manifold designs previously. In the gas (air) phase, the spacing between fins, fin dimensions and positioning of the pipes within the fin design, as well as the combined influence of these individual characteristics is novel in that this design uses extended surfaces to boost the heat transfer capability of the device whilst reducing the overall volume, ultimately increasing the power density beyond that seen in traditional radiator systems. Due to manufacturing constraints at the time, flat fins were fixed to the heat pipes which limit the effective heat transfer surface area on the air-side of the HEX. Alleviating this limitation by corrugating the fins thus significantly increasing the surface area within the same volume is being explored.

6 ACKNOWLEDGEMENTS

We gratefully acknowledge the support from Enterprise Ireland under the grant CFTD -07 -IT -307.

7 REFERENCES

[1]. R. Rawlings, Energy Efficiency Best Practice in Housing Domestic Ground Source Heat Pumps: Design and installation of closed-loop systems March 2004. Energy Saving Trust. E&OE. CE82.

[2]. ASHRAE. Systems and Equipment Handbook, American Society of Heating, Refrigerating and Air Conditioning Engineers, 1996.

[3]. CIBSE. 2006. Guide A: Environmental design, 7^{th} Edition London, Chartered Institution of Building Services Engineers.

[4]. Hydronic System Design & Operation, A Guide to Heating & Cooling with Water, Erwin G Hansen, McGraw-Hill Publishing Company. 1985

[5]. C.J. Savage, Heat pipes and vapour chambers for satellite thermal balance. RAE Tech. Report 69125, June 1969.

[6]. T.D. Swanson. G.C. Birur. NASA thermal control technologies for robotic spacecraft. Applied Thermal Engineering, 23, (2003) 1055–1065.

[7]. A. Caruso, et al. Heat pipe heat storage performance. Heat Recovery Systems CHP, 9(5) (1989) 407–410.

[8]. B. Zalba. J.M. Marin. L.F. Cabeza. H. Mehling, Review on thermal energy storage with phase change: materials, heat transfer analysis and applications. Applied Thermal Engineering, 23 (2003) 251–283.

[9]. M.S. Sodha, N.K. Bansal, P. k. Bansal, A. Kumar, M.A.S. Malik, Solar Passive Building: Science and Design. Pergamon, Oxford, 1986.

[10]. E. Mathioulakis. V. Belessiotis, A new Heat-pipe Type Solar Domestic Hot Water System, Solar Energy, 72(1), (2002) 13-20.

[11]. Q.P. Sun. X.H. Chen. J. F. Chen, The Development and Application of Solar Energy Heat-pipe, Energy Technology, 23 (3), (2002) 110-112.

[12]. L.L. Vasiliev, Heat pipe research and development in the USSR. Heat Recovery Systems. CHP, 9 (4), (1989) 313–333.

[13]. H. Jouhara, Economic Assessment of the Benefits of Wraparound Heat Pipes in Ventilation Processes for Hot and Humid Climates, International Journal of Low Carbon Technology, 4 (1), (2009) 52-60.

[14]. H. Jouhara, R. Meskimmon, Experimental investigation of wraparound loop heat pipe heat exchanger used in energy efficient air handling units, Energy (2010), doi:10.1016/j.energy.2010.03.056

[15]. D. Reay, P. Kew, (5th Ed.), Heat Pipes, USA: Butterworth-Heinemann.; 2006

[16]. A. Faghri, (1st Ed.), Heat Pipe Science and Technology, Taylor & Francis, 1995.

[17]. Kempers, R., Robinson, A.J., Ewing, D., and Ching, C.Y., (2008) “Characterization of Evaporator and Condenser Thermal Resistances of a Screen Mesh Wicked Heat Pipe,” International Journal of Heat and Mass Transfer, 51 (25-26), pp. 6039-6046.

[18]. H. Jouhara. A.J. Robinson, An experimental study of small diameter wickless heat pipes operating in the temperature range 200ºC to 450ºC, Heat Transfer Engineering, 30 (13), (2009) pp. 1041 - 1048.

[19]. H. Jouhara, A.J. Robinson, Experimental investigation of small diameter two-phase closed thermosyphons charged with water, FC-84, FC-77 and FC-3283, Appl. Therm. Eng. (2009), doi:10.1016/j.applthermaleng.2009.08.007.